Articles

Effects of Main-Group and Transition Elements on Bond Formation and Cleavage in Transition-Metal Chalcogenide Clusters: Reactions of $E_2Fe_3(CO)_9$ (E = Te, Se) with $[Co(CO)_4]^-$, $[Mn(CO)_5]^-$, and $[Fe(CO)_4]^{2-}$

Minghuey Shieh* and Tse-Fang Tang

Department of Chemistry, National Taiwan Normal University, Taipei 11718, Taiwan, Republic of China

Shie-Ming Peng and Gene-Hsiang Lee

Department of Chemistry, National Taiwan University, Taipei 10764, Taiwan, Republic of China

Received November 4, 1994[⊗]

The tetrahedral clusters $[EFe_2Co(CO)_9]^-$ (E = Te, **I**; E = Se, **II**) were synthesized by reactions of the isostructural complexes $E_2Fe_3(CO)_9$ with $[Co(CO)_4]^-$, respectively. Reaction of $Te_2Fe_3(CO)_9$ with $[Mn(CO)_5]^-$ gives a $Mn(CO)_4$ bridging butterfly $[Te_2Fe_2Mn(CO)_{10}]^-$ (**III**), while treatment of $Se_2Fe_3(CO)_9$ with $[Mn(CO)_5]^-$ produces a square-pyramidal $[Se_2Fe_2Mn(CO)_9]^-$ (**IV**). When $Te_2Fe_3(CO)_9$ reacts with Collman's reagent, $[Fe(CO)_4]^{2-}$ the previously characterized $[Te_6Fe_8(CO)_{24}]^{2-}$ is formed. The similar reaction of $Se_2Fe_3(CO)_9$ with $[Fe(CO)_4]^{2-}$ generates the known complexes $[SeFe_3(CO)_9]^{2-}$ and $[HSeFe_3(CO)_9]^-$. The anionic complexes **I-IV** are fully characterized by infrared spectroscopy, elemental analysis, negative-ion mass, or/and X-ray diffraction methods. Crystals of $[Et_4N]$-[**II**] are tetragonal, space group $P4_2/ncm$ with a = 16.456(3) Å, c = 17.925(6) Å, V = 4854(2) Å^3, Z = 8, R = 0.045, and R_w = 0.051 at 25 °C. $[Et_4N]$[**III**] crystallizes in the triclinic space group $P\bar{1}$ with a = 9.343(3) Å, b = 12.401(6) Å, c = 13.198(2) Å, α = 77.96(3)°, β = 74.36(2)°, γ = 69.72(3)°, V = 1370(1) Å^3, Z = 2, R = 0.026, and R_w = 0.028 at 25 °C. Crystals of $[Et_4N]$[**IV**] are monoclinic, space group $P2_1/n$ with a = 9.236(2) Å, b = 24.665(6) Å, c = 11.870(1) Å, β = 112.62(2)°, V = 2496(1) Å^3, Z = 4, R = 0.032, and R_w = 0.039 at 25 °C. This paper describes the similarities and differences among these reactions and discusses the effects of the main-group and transition elements on bond formation and cleavage of transition-metal chalcogenide clusters.

Introduction

Iron−chacogenide carbonyl complexes have attracted extensive attention due to their potential uses as solid state precursors and their versatile bonding modes and reactivity patterns.[1,2] It is suggested that the chemistry of tellurides may prove distinctive from that of their selenium analogues due to the increased size and enhanced acidity of the tellurium atom. Recently, the square-pyramidal complexes $E_2Fe_3(CO)_9$ (E = Te, Se) were found to be effective in the cluster-building reactions.[3] The role of tellurium in cluster assemblies has been discussed by Rauchfuss and co-workers, and several related reactions were performed to probe their mechanisms of formation.[4,5]

It has been shown that the reactions of $Te_2Fe_3(CO)_9$ with the Lewis bases such as PPh_3 behave differently from those of their sulfur and selenium analogues attributable to the Lewis acidity of Te.[6,7] Parallel results are obtained when $E_2Fe_3(CO)_9$ (E = Te, Se) are treated with transition-metal complexes such as $M(PPh_3)_4$ (M = Ni, Pt, Pd).[8,9] Nevertheless, there is still a lack of systematic investigation and comparison of the effects of the main-group and transition elements on the formation of mixed main-group element−transition-metal clusters.

The key factors influencing the formation of main-group element−transition metal clusters may depend on the effect of the main-group element on the mixed-metal clusters, the nature of the bonding between the main-group and transition elements, and the ease of the bond formation between main-group elements and between transition-metal elements. With the objective of evaluating these effects, we examine the reductive

* To whom all correspondence should be addressed.

[⊗] Abstract published in *Advance ACS Abstracts,* May 1, 1995.

(1) (a) Ansari, M. A.; Ibers, J. A. *Coord. Chem. Rev.* **1990**, *100*, 223. (b) Coucouvanis, D. *Acc. Chem. Res.* **1991**, *24*, 1.
(2) (a) Eichhorn, B. W.; Haushalter, R. C. *Inorg. Chem.* **1990**, *29*, 728. (b) Bogan, L. E., Jr.; Lesch, D. A.; Rauchfuss, T. B. *J. Organomet. Chem.* **1983**, *250*, 429. (c) Adams, R. D.; Babin, J. E.; Wang, J. G.; Wu, W. *Inorg. Chem.* **1989**, *28*, 703. (d) Adams, R. D.; Babin, J. E.; Tsai, M. *Inorg. Chem.* **1987**, *26*, 2807. (e) Adams, R. D. *Polyhedron* **1985**, *4*, 2003. (f) Mathur, P.; Mavunkal, I. J.; Rheingold, A. L. *J. Chem. Soc., Chem. Commun.* **1989**, 382. (g) Roof, L. C.; Pennington, W. T.; Kolis, J. W. *J. Am.Chem. Soc.* **1990**, *112*, 8172. (h) Roof, L. C.; Kolis, J. W. *Chem. Rev.* **1993**, *93*, 1037.
(3) Ward, M. D. *Coord. Chem. Rev.* **1992**, *115*, 1.
(4) Bogan, L. E., Jr.; Rauchfuss, T. B.; Rheingold, A. L. *J. Am. Chem. Soc.* **1985**, *107*, 3843.
(5) Bogan, L. E., Jr.; Clark, G. R.; Rauchfuss, T. B. *Inorg. Chem.* **1986**, *25*, 4050.
(6) (a) Cetini, G.; Stanghellini, P. L.; Rossetti, R.; Gambino, O. *J. Organomet. Chem.* **1968**, *15*, 373. (b) Cetini, G.; Stanghellini, P. L.; Rossetti, R.; Gambino, O. *Inorg. Chim. Acta* **1968**, *2*, 433. (c) Rossetti, R.; Stanghellini, P. L.; Gambino, O.; Cetini, G. *Inorg. Chim. Acta* **1972**, *6*, 205. (d) Stanghellini, P. L.; Cetini, G.; Gambino, O.; Rossetti, R. *Inorg. Chim. Acta* **1968**, *3*, 651. (e) Aime, S.; Milone, L.; Rossetti, R.; Stanghellini, P. L. *J. Chem. Soc., Dalton Trans.* **1980**, 46. (f) Rossetti, R.; Stanghellini, P. L. *J. Coord. Chem.* **1974**, *3*, 217.
(7) Lesch, D. A.; Rauchfuss, T. B. *Organometallics* **1982**, *1*, 499.
(8) Mathur, P.; Mavunkal, I. J. *J. Organomet. Chem.* **1988**, *350*, 251.
(9) Mathur, P.; Mavunkal, I. J.; Rugmini, V. *J. Organomet. Chem.* **1989**, *367*, 243.

0020-1669/95/1334-2797$09.00/0

behaviors of clusters $E_2Fe_3(CO)_9$ (E = Te, Se) toward a series of transition-metal anions $[Co(CO)_4]^-$, $[Mn(CO)_5]^-$, and $[Fe(CO)_4]^{2-}$. This work describes the similarities and differences among these reactions, provides facile and rational routes to transition-metal chalcogenide clusters, and highlights the effects of the main-group and transition-metal elements on the cluster formation.

Experimental Section

All reactions were performed under an atmosphere of pure nitrogen by using standard Schlenk line techniques. Solvents were purified, dried, and distilled under nitrogen prior to use. $Co_2(CO)_8$ (Strem), $Fe(CO)_5$ (Aldrich), $Mn_2(CO)_{10}$ (Strem), $K_2TeO_3{\cdot}H_2O$ (Alfa), SeO_2 (Strem), $[Et_4N]Br$ (Merck), [PPN]Cl (Aldrich), and $[PhCH_2NMe_3]Cl$ (Aldrich) were used as received. Infrared spectra were recorded on a Jasco 700 IR spectrometer using CaF_2 liquid cells. ESI mass spectra were obtained on a Fision (VG platform) mass spectrometer. Elemental analyses were performed at the NSC Regional Instrumentation Center at National Taiwan University, Taipei, Taiwan, or National Tsing Hua University, Hsinchu, Taiwan. $E_2Fe_3(CO)_9$ (E = Se, Te),[10,11] $Na[Co(CO)_4]$,[12] and $Na_2Fe(CO)_4$[13] were prepared by the published methods.

Reaction of $Te_2Fe_3(CO)_9$ with $[Co(CO)_4]^-$. Following a published procedure for synthesis of $Na[Co(CO)_4]$, 1.10 g (3.2 mmol) of $Co_2(CO)_8$ was treated with 1.5 g (37.5 mmol) of powdered NaOH in 40 mL of THF. The freshly made $Na[Co(CO)_4]$ solution was added to 2.3 g (3.4 mmol) of $Te_2Fe_3(CO)_9$. The mixed solution wrapped with aluminum foil was stirred at room temperature for 14 days. The solution was filtered, and solvent was removed under vacuum. The residue was then dissolved in 5 mL of MeOH, and an excess amount of $[Et_4N]Br$ was added to give the precipitate. The solid was washed with H_2O and dried under vacuum overnight. The residue was washed with hexanes to remove the unreacted $Te_2Fe_3(CO)_9$ and then extracted with ether to give 0.99 g (1.45 mmol) of $[Et_4N][TeFe_2Co(CO)_9]$ ($[Et_4N]$[**I**]) (43% based on the starting $Te_2Fe_3(CO)_9$). $[Et_4N]$[**I**] is soluble in ether, CH_2Cl_2, and THF but insoluble in hexanes. IR (ν_{CO}, ether) for $[Et_4N]$[**I**]: 2046 m, 1992 s, 1961 m, br cm^{-1}. ESI-MS for negative ion: *m/e* 552.5. Anal. Calcd (found) for $[Et_4N]$[**I**]: C, 30.0 (30.79); H, 2.96 (3.04); N, 2.06 (2.22); Fe, 16.41 (16.6); Co, 8.66 (8.70).

Reaction of $Se_2Fe_3(CO)_9$ with $[Co(CO)_4]^-$. Following a published procedure for synthesis of $Na[Co(CO)_4]$, 0.70 g (2.0 mmol) of $Co_2(CO)_8$ was treated with 1.0 g (25 mmol) of powdered NaOH in 40 mL of THF. The freshly made $Na[Co(CO)_4]$ solution was added into 1.2 g (2.1 mmol) of $Se_2Fe_3(CO)_9$. The mixed solution wrapped with aluminum foil was stirred at room temperature for 24 days. The solution was filtered, and solvent was removed under vacuum. The residue was then dissolved in 5 mL of MeOH, and an excess amount of $[Et_4N]Br$ was added to give the precipitate. The solid was washed with H_2O and dried under vacuum overnight. The residue was washed with hexanes to remove the unreacted $Se_2Fe_3(CO)_9$ and then extracted with ether to give 0.82 g (1.30 mmol) of $[Et_4N][SeFe_2Co(CO)_9]$ ($[Et_4N]$[**II**]) (62% based on the starting $Se_2Fe_3(CO)_9$). Crystals suitable for X-ray diffraction were grown from hexanes/ether/CH_2Cl_2 solution. $[Et_4N]$[**II**] is soluble in ether, CH_2Cl_2, and THF but insoluble in hexanes. IR (ν_{CO}, CH_2Cl_2) for $[Et_4N]$[**II**]: 2052 m, 1990 s, 1965 sh, 1930 m, br cm^{-1}. ESI-MS for negative ion: *m/e* 502.6. Anal. Calcd (found) for $[Et_4N]$[**II**]: C, 32.31 (32.18); H, 3.19 (3.18); N, 2.22 (2.12); Fe, 17.67 (18.5); Co, 9.33 (9.52).

Synthesis of $[Et_4N][Mn(CO)_5]$. To a mixture of 1.8 g (4.6 mmol) of $Mn_2(CO)_{10}$ and 0.8 g (4.4 mmol) of Ph_2CO was added 60 mL of THF. A quantity of 0.1 g (4.3 mmol) of Na was then added to the mixed solution, and the solution turned blue-purple. The solution was stirred at room temperature for 1 h, filtered, and dried under vacuum. The residue was redissolved in MeOH, and 0.96 g (4.6 mmol) of $[Et_4N]$Br was added to give a mixed solution. The solution was stirred for 1 h and then filtered and dried under vacuum. The residue was washed with hexanes, ether, and H_2O and dried under vacuum overnight. The solid was extracted with CH_2Cl_2 to give 2.44 g (7.50 mmol) of $[Et_4N][Mn(CO)_5]$ (82% based on Mn). IR (ν_{CO}, CH_2Cl_2) for $[Et_4N][Mn(CO)_5]$: 1901 s, 1861 s cm^{-1}.

Reaction of $Te_2Fe_3(CO)_9$ with $[Mn(CO)_5]^-$. To a mixture of 0.62 g (0.92 mmol) of $Te_2Fe_3(CO)_9$ and 0.30 g (0.92 mmol) of $[Et_4N][Mn(CO)_5]$ was added 60 mL of CH_2Cl_2. The solution was stirred at room temperature for 2 days and then filtered, and solvent was removed under vacuum. The residue was then washed with hexanes and extracted with ether/THF (20/1 v/v) to give a reddish brown solution. The product was collected by precipitating it with hexanes to give 0.68 g (0.817 mmol) of $[Et_4N][Te_2Fe_2Mn(CO)_{10}]$ ($[Et_4N]$[**III**]) (89% based on the starting $Te_2Fe_3(CO)_9$). $[Et_4N]$[**III**] is sparingly soluble in ether and soluble in CH_2Cl_2 and THF but insoluble in hexanes. IR (ν_{CO}, ether) for $[Et_4N]$[**III**]: 2050 m, 2017 vs, 1990 vs, 1952 s, 1923 sh cm^{-1}. ESI-MS for negative ion: *m/e* 706.4. Anal. Calcd (found) for $[Et_4N]$[**III**]: C, 25.98 (26.02); H, 2.42 (2.40); N, 1.68 (1.57); Fe, 13.42 (11.3); Mn, 6.60 (5.93).

Reaction of $Se_2Fe_3(CO)_9$ with $[Mn(CO)_5]^-$. To a mixture of 0.76 g (1.32 mmol) of $Se_2Fe_3(CO)_9$ and 0.43 g (1.32 mmol) of $[Et_4N][Mn(CO)_5]$ was added 60 mL of CH_2Cl_2. The solution was stirred at room temperature for 4 days and then filtered, and solvent was removed under vacuum. The residue was then washed with hexanes and extracted with ether to give a brown solution, and hexanes were added to the solution giving 0.71 g (1.00 mmol) of $[Et_4N][Se_2Fe_2Mn(CO)_9]$ ($[Et_4N]$[**IV**]) (76% based on the starting $Se_2Fe_3(CO)_9$). $[Et_4N]$[**IV**] is soluble in ether, CH_2Cl_2, and THF but insoluble in hexanes. IR (ν_{CO}, CH_2Cl_2) for $[Et_4N]$[**IV**]: 2048 m, 2000 vs, 1981 vs, 1894 m cm^{-1}. ESI-MS for negative ion: *m/e* 578.6. Anal. Calcd (found) for $[Et_4N]$[**IV**]: C, 28.88 (28.90); H, 2.85 (2.90); N, 1.98 (1.89); Fe, 15.80 (15.5); Mn, 7.77 (7.45).

Reaction of $Te_2Fe_3(CO)_9$ with $[Fe(CO)_4]^{2-}$. To a mixture of 2.0 g (3.0 mmol) of $Te_2Fe_3(CO)_9$ and 0.70 g (3.2 mmol) of $Na_2Fe(CO)_4$ was added 40 mL of CH_2Cl_2. The mixed solution was stirred at room temperature for 10 days and then filtered and dried under vacuum. The residue was redissolved in MeOH, and 0.70 g (3.3 mmol) of $[Et_4N]$Br in H_2O was added to yield the precipitate. The solid was then collected, washed with H_2O, and dried under vacuum overnight. The residue was then washed with hexanes and extracted with CH_2Cl_2 to give 0.85 g (0.40 mmol) of $[Et_4N]_2[Te_6Fe_8(CO)_{24}]$ (40% based on Te). IR (ν_{CO}, CH_2Cl_2) for $[Et_4N]_2[Te_6Fe_8(CO)_{24}]$: 2027 s, 2006 s, 1959 m cm^{-1}.

Reaction of $Se_2Fe_3(CO)_9$ with $[Fe(CO)_4]^{2-}$. To a mixture of 0.5 g (0.87 mmol) of $Se_2Fe_3(CO)_9$ and 0.20 g (0.94 mmol) of $Na_2Fe(CO)_4$ was added 60 mL of THF. The mixed solution was stirred at room temperature for 5 days and then filtered and dried under vacuum. The residue was redissolved in MeOH, and 0.4 g (1.9 mmol) of $[Et_4N]$Br in H_2O was added to yield the precipitate. The solid was then collected, washed with H_2O, and dried under vacuum overnight. The residue was then washed with hexanes and extracted with ether to give 0.125 g (0.20 mmol) of $[Et_4N][HSeFe_3(CO)_9]$ (23% based on the starting $Se_2Fe_3(CO)_9$). IR (ν_{CO}, CH_2Cl_2) for $[Et_4N][HSeFe_3(CO)_9]$: 2038 w, 2010 s, 1981 s, 1963 m, 1909 w, br cm^{-1}.[15] The residue was then extracted into CH_2Cl_2 to give a small amount of the known complex $[Et_4N]_2[SeFe_3(CO)_9]$.[10,14] IR (ν_{CO}, MeCN) for $[Et_4N]_2[SeFe_3(CO)_9]$: 1966 w, 1928 s, 1901 m, 1873 w cm^{-1}.

X-ray Structural Characterization of $[Et_4N]$[II], $[Et_4N]$[III], and $[Et_4N]$[IV]. A summary of selected crystallographic data for $[Et_4N]$[**II**], $[Et_4N]$[**III**], and $[Et_4N]$[**IV**] is given in Table 1. Data collection was carried out on a Nonius CAD-4 diffractometer using graphite-monochromated Mo Kα radiation at 25 °C. All crystals were mounted on glass fibers with epoxy cement. Data reduction and structural refinement were performed using the NRCC−SDP−VAX packages,[16] and atomic scattering factors were taken from ref 17.

Reddish-black crystals of $[Et_4N]$[**II**] suitable for X-ray analysis were grown from hexanes/ether/CH_2Cl_2 solution. A total of 1688 unique

(10) Shieh, M.; Tsai, Y.-C. *Inorg. Chem.* **1994**, *33*, 2303.
(11) Lesch, D. A.; Rauchfuss, T. B. *Inorg. Chem.* **1981**, *20*, 3583.
(12) Edgell, W. F.; Lyford, J. *Inorg. Chem.* **1970**, *9*, 1932.
(13) Collman, J. P.; Finke, R. G.; Cawse, J. N.; Brauman, J. I. *J. Am. Chem. Soc.* **1977**, *99*, 2515.
(14) Bachman, R. E.; Whitmire, K. H. *Inorg. Chem.* **1994**, *33*, 2527.
(15) Shieh, M.; Tsai, Y.-C. Unpublished results.
(16) Gabe, E. J.; Lepage, Y.; Charland, J. P.; Lee, F. L.; White, P. S. *J. Appl. Crystallogr.* **1989**, *22*, 384.
(17) *International Tables for X-ray Crystallography*; Kynoch Press: Birmingham, 1974; Vol. IV.

Table 1. Selected Crystallographic Data for $[Et_4N][SeFe_2Co(CO)_9]$ ($[Et_4N]$[**II**]), $[Et_4N][Te_2Fe_2Mn(CO)_{10}]$ ($[Et_4N]$[**III**]), and $[Et_4N][Se_2Fe_2Mn(CO)_9]$ ($[Et_4N]$[**IV**])

	$[Et_4N]$[**II**]	$[Et_4N]$[**III**]	$[Et_4N]$[**IV**]
empirical formula	$SeFe_2CoC_{17}O_9H_{20}N$	$Te_2Fe_2MnC_{18}O_{10}H_{20}N$	$Se_2Fe_2MnC_{17}O_9H_{20}N$
fw	631.93	832.19	707.81
cryst system	tetragonal	triclinic	monoclinic
space group	$P4_2/ncm$	$P\bar{1}$	$P2_1/n$
a, Å	16.456(3)	9.343(3)	9.236(2)
b, Å		12.401(6)	24.665(6)
c, Å	17.925(6)	13.198(2)	11.870(1)
α, deg		77.96(3)	
β, deg		74.36(2)	112.62(2)
γ, deg		69.72(3)	
V, Å^3	4854(2)	1370(1)	2496(1)
Z	8	2	4
D(calc), g cm^{-3}	1.729	2.017	1.830
abs coeff, cm^{-1}	33.8	36.2	46.5
diffractometer	Nonius (CAD-4)	Nonius (CAD-4)	Nonius (CAD-4)
radiation, λ(Mo Kα), Å	0.7107	0.7107	0.7107
temp, °C	25	25	25
T_{min}/T_{max}	0.74/1.00	0.60/1.00	0.63/1.00
residuals: R;[a] R_w[a]	0.045; 0.051	0.026; 0.028	0.032; 0.039

[a] The functions minimized during least-squares cycles were $R = \sum|F_o - F_c|/\sum F_o$ and $R_w = [\sum w(F_o - F_c)^2/\sum w(F_o)^2]^{1/2}$.

Table 2. Selected Atomic Coordinates and Isotropic Displacement Coefficients (Å^2) for $[Et_4N][SeFe_2Co(CO)_9]$ ($[Et_4N]$[**II**])

	x	y	z	B_{eq}
Se	0.92588(6)	0.57412	0.2191(1)	5.53(6)
Co	0.96182(9)	0.53818	0.3382(1)	5.25(8)
Fe	0.95189(9)	0.43737(9)	0.22880(8)	4.69(6)
C(1)	1.0225(7)	0.4775	0.3960(8)	6.3(7)
C(2)	0.8679(7)	0.5190(7)	0.3794(7)	7.1(7)
C(3)	1.0118(6)	0.3618(6)	0.2693(6)	5.5(6)
C(4)	0.8529(7)	0.3992(6)	0.2522(7)	6.5(6)
C(5)	0.9592(8)	0.4083(8)	0.1349(7)	8.0(7)
O(1)	1.0612(5)	0.4388	0.4369(6)	9.4(5)
O(2)	0.8049(6)	0.5086(7)	0.4066(6)	11.0(6)
O(3)	1.0489(5)	0.3098(5)	0.2961(5)	8.1(5)
O(4)	0.7913(4)	0.3742(5)	0.2667(6)	9.7(6)
O(5)	0.9657(8)	0.3877(7)	0.0735(5)	12.7(8)

reflections were collected and corrected for absorption and decay.[16] The structure of $[Et_4N]$[**II**] was solved by the heavy-atom method and refined by least-squares cycles. The heavy atoms and all other non-hydrogen atoms were refined with anisotropic thermal parameters. Full-matrix least-squares refinement of $[Et_4N]$[**II**] led to convergence with $R = 4.5\%$ and $R_w = 5.1\%$ for those reflections with $I > 2.0\sigma(I)$.

Reddish-brown crystals of $[Et_4N]$[**III**] suitable for X-ray analysis were grown from CH_2Cl_2 solution. A total of 3591 unique reflections were collected for $[Et_4N]$[**III**] and corrected for absorption and decay. The structure of $[Et_4N]$[**III**] was solved by direct methods which indicated the presence of Te and Fe atoms. The light atoms were found using successive least-squares cycles and difference Fourier maps. All non-hydrogen atoms were refined with anisotropic thermal parameters. Full-matrix least-squares refinement of $[Et_4N]$[**III**] led to convergence with $R = 2.6\%$ and $R_w = 2.8\%$, respectively, for those reflections with $I > 2.0\sigma(I)$.

Reddish-brown crystals of $[Et_4N]$[**IV**] suitable for X-ray analysis were grown from hexanes/CH_2Cl_2 solution. A total of 3254 unique reflections were collected and corrected for absorption and decay. The structure of $[Et_4N]$[**IV**] was solved by the heavy-atom method and refined by least-squares cycles. For the anion, one iron and one manganese atoms were found disordered and all other non-hydrogen atoms were refined with anisotropic thermal parameters. The cation was solved by fixed flag refinement because of the disorder problem. Full-matrix least-squares refinement of $[Et_4N]$[**IV**] led to convergence with $R = 3.2\%$ and $R_w = 3.9\%$ for those reflections with $I > 2.0\sigma(I)$.

The selected atomic coordinates of $[Et_4N]$[**II**], $[Et_4N]$[**III**], and $[Et_4N]$[**IV**] are given in Tables 2–4, respectively. Selected bond distances and angles of $[Et_4N]$[**II**] are presented in Table 5, those of $[Et_4N]$[**III**] are listed in Table 6, and those of $[Et_4N]$[**IV**] are given in Table 7. Additional crystallographic data are available as supplementary material.

Results

Reaction of $E_2Fe_3(CO)_9$ (E = Te, Se) with $[Co(CO)_4]^-$, $[Mn(CO)_5]^-$, and $[Fe(CO)_4]^{2-}$. Reactions of $E_2Fe_3(CO)_9$ (E = Te, Se) with $[Co(CO)_4]^-$ form two new tetrahedral metal clusters $[EFe_2Co(CO)_9]^-$ (E = Te, **I**; Se, **II**), respectively. The infrared spectra of clusters **I** and **II** show similar absorptions characteristic of the terminal carbonyl ligands in the region 2052–1930 cm^{-1}, and the pattern is similar to those for the tetrahedral complexes $[EFe_3(CO)_9]^{2-}$ (E = S, Se).[10,14,18] The elemental analysis and negative-ion mass methods confirm their formula as $[EFe_2Co(CO)_9]^-$ (E = Te, Se). $[Et_4N]$[**II**] is further structurally characterized by the single-crystal X-ray diffraction method. Unfortunately, attempts at X-ray structural determination of the anion **I** have been thwarted due to severe disorder problems. Nevertheless, $[Et_4N]$[**I**] is believed to be isostructural to $[Et_4N]$[**II**] on the basis of similar IR absorption patterns, elemental analysis, and mass spectroscopy.

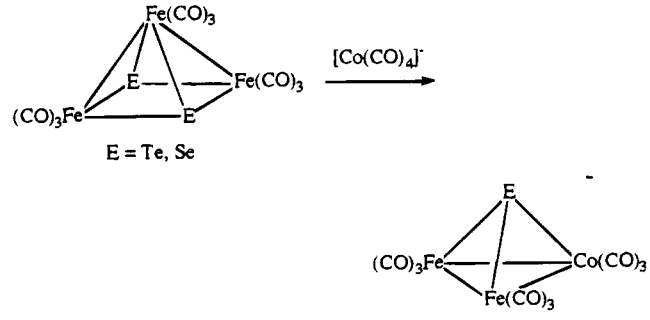

To compare to the reactions with $[Co(CO)_4]^-$, it was interesting to know if similar heterometal systems might be produced by using other transition-metal anions such as $[Mn(CO)_5]^-$. When $Te_2Fe_3(CO)_9$ is treated with $[Mn(CO)_5]^-$, a $[Mn(CO)_4]$ fragment bridging butterfly anion $[Te_2Fe_2Mn(CO)_{10}]^-$ (**III**) is formed. The formulation of **III** is substantiated by elemental analysis and negative-ion mass spectroscopy. The infrared spectrum of **III** indicates that only terminal CO ligands are present. An X-ray analysis reveals that **III** adopts an *arachno*-Te_2Fe_2Mn structure. Oxidation of cluster **III** leads to the loss of manganese fragment and the formation of the known cluster $Te_2Fe_3(CO)_9$. On the other hand, the reaction of Se_2-

(18) Markó, L.; Takács, J.; Rapp, S.; Markó-Monostory, B. *Inorg. Chim. Acta Lett.* **1980**, *45*, L189.

Table 3. Selected Atomic Coordinates and Isotropic Displacement Coefficients (Å^2) for $[Et_4N][Te_2Fe_2Mn(CO)_{10}]$ ($[Et_4N]$[**III**])

	x	*y*	*z*	B_{eq}
Te(1)	0.52302(4)	0.33680(3)	0.17631(3)	3.41(2)
Te(2)	0.55736(5)	0.10917(3)	0.34768(3)	4.12(2)
Fe(1)	0.5175(1)	0.31885(7)	0.37650(7)	3.95(5)
Fe(2)	0.76565(9)	0.21147(7)	0.25019(6)	3.33(4)
Mn	0.3988(1)	0.1674(8)	0.19178(8)	4.03(5)
C(1)	0.3189(7)	0.3787(5)	0.4332(5)	4.9(4)
C(2)	0.5708(8)	0.4452(6)	0.3590(5)	5.9(4)
C(3)	0.5815(8)	0.2659(6)	0.4961(5)	6.5(4)
C(4)	0.8457(7)	0.3277(5)	0.2089(5)	4.4(3)
C(5)	0.8773(7)	0.1406(5)	0.3496(5)	4.6(3)
C(6)	0.8881(7)	0.1247(5)	0.1497(5)	4.1(3)
C(7)	0.5773(7)	0.0880(5)	0.1047(5)	4.9(4)
C(8)	0.3263(7)	0.0455(6)	0.2233(6)	5.8(4)
C(9)	0.3074(7)	0.2271(6)	0.0809(6)	5.5(4)
C(10)	0.2288(7)	0.2465(6)	0.2843(5)	5.2(4)
O(1)	0.1915(5)	0.4277(4)	0.4744(4)	7.3(3)
O(2)	0.6031(7)	0.5281(5)	0.3510(5)	9.9(4)
O(3)	0.6222(7)	0.2314(5)	0.5751(4)	10.6(4)
O(4)	0.8970(5)	0.4026(4)	0.1809(4)	6.7(3)
O(5)	0.9511(5)	0.0967(4)	0.4117(4)	6.9(3)
O(6)	0.9757(5)	0.0716(4)	0.0860(4)	6.5(3)
O(7)	0.6840(5)	0.0349(4)	0.0491(4)	7.2(3)
O(8)	0.2844(7)	-0.0336(4)	0.2378(5)	9.3(4)
O(9)	0.2488(6)	0.2654(5)	0.0098(4)	8.4(4)
O(10)	0.1184(5)	0.2964(4)	0.3402(4)	7.3(3)

Table 4. Selected Atomic Coordinates and Isotropic Displacement Coefficients (Å^2) for $[Et_4N][Se_2Fe_2Mn(CO)_9]$ ($[Et_4N]$[**IV**]) (Where M = $^1/_2$Mn + $^1/_2$Fe)

	x	*y*	*z*	B_{eq}
Se(1)	0.59383(8)	0.39170(3)	0.19243(7)	3.47(3)
Se(2)	0.71884(8)	0.32773(3)	0.43794(6)	3.25(3)
M(1)	0.8431(1)	0.39486(4)	0.3598(1)	3.51(5)
M(2)	0.4624(1)	0.33515(5)	0.2844(1)	3.50(5)
Fe(3)	0.7057(1)	0.30331(4)	0.23970(9)	3.03(5)
C(1)	0.820(1)	0.4529(3)	0.4385(8)	4.7(4)
C(2)	0.9306(9)	0.4326(3)	0.2730(7)	4.5(4)
C(3)	1.0329(9)	0.3793(4)	0.4754(8)	4.8(4)
C(4)	0.3928(9)	0.3866(4)	0.3533(8)	4.8(4)
C(5)	0.299(1)	0.3308(4)	0.1430(8)	6.0(5)
C(6)	0.4064(9)	0.2767(4)	0.3464(9)	5.3(5)
C(7)	0.614(1)	0.2862(3)	0.0850(7)	4.7(4)
C(8)	0.712(1)	0.2346(3)	0.2844(7)	4.5(4)
C(9)	0.902(1)	0.3085(3)	0.2447(8)	4.8(5)
O(1)	0.8020(9)	0.4900(3)	0.4896(7)	7.7(4)
O(2)	0.9840(8)	0.4572(3)	0.2167(6)	7.4(4)
O(3)	1.1521(7)	0.3698(3)	0.5501(6)	7.8(4)
O(4)	0.3523(9)	0.4211(3)	0.3989(7)	7.4(4)
O(5)	0.1918(8)	0.3301(4)	0.0540(6)	10.1(6)
O(6)	0.3724(8)	0.2401(3)	0.3893(8)	8.6(5)
O(7)	0.5570(9)	0.2741(3)	-0.0165(6)	7.8(4)
O(8)	0.7125(9)	0.1897(2)	0.3094(6)	7.3(5)
O(9)	1.0203(7)	0.3046(3)	0.2360(8)	7.8(5)

Table 5. Selected Bond Distances (Å) and Bond Angles (deg) for $[Et_4N][SeFe_2Co(CO)_9]$ ($[Et_4N]$[**II**])

(A) Distances: Metal−Metal Bond Lengths			
Se−Co	2.293(3)	Se−Fe	2.297(2)
Co−Fe	2.573(2)	Fe−Fe	2.577(3)
(B) Bond Angles			
Co−Se−Fe	68.20(7)	Fe−Se−Fe	68.24(7)
Se−Co−Fe	55.98(5)	Fe−Co−Fe	60.10(6)
Se−Fe−Co	55.82(8)	Se−Fe−Fe	55.88(5)
Co−Fe−Fe	59.95(6)		

$Fe_3(CO)_9$ with $[Mn(CO)_5]^-$ forms a square-pyramidal *nido*-cluster $[Se_2Fe_2Mn(CO)_9]^-$ (**IV**). X-ray analysis shows that it is not possible to distinguish the positions of the iron and manganese atoms. However, elemental analysis, negative-ion MS, and the electron-counting rules confirm its formula.

Comparing the structures of **III** and **IV** leads to an obvious question if the *arachno*-cluster **III** can lose one carbonyl group to form a *nido*-cluster $[Te_2Fe_2Mn(CO)_9]^-$ structurally analogous to **IV**. To answer this, an independent experiment was conducted. It was found when $[Et_4N]$[**III**] was refluxed in THF no other cluster was observed. It indicates that $[Et_4N]$[**III**] is a thermodynamically stable product and its conversion to a square-pyramidal cluster does not occur under our reaction conditions.

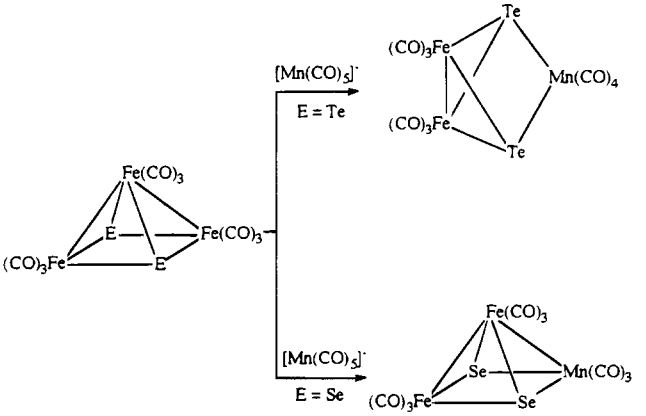

For comparison, the reactions of $E_2Fe_3(CO)_9$ (E = Te, Se) with the dianion $[Fe(CO)_4]^{2-}$ were further investigated. Unexpectedly, treatment of $Te_2Fe_3(CO)_9$ with $[Fe(CO)_4]^{2-}$ produces the previously reported cluster $[Te_6Fe_8(CO)_{24}]^{2-}$, which consists of a $[Te_2Fe_2(CO)_6]^{2-}$ anion and two $Te_2Fe_3(CO)_9$ clusters.[19] In the reaction of $Se_2Fe_3(CO)_9$ with $[Fe(CO)_4]^{2-}$, a mixture of the dianion $[SeFe_3(CO)_9]^{2-}$ and the monoanion $[HSeFe_3(CO)_9]^-$ is found. We have noted that $[SeFe_3(CO)_9]^{2-}$ can convert to $[HSeFe_3(CO)_9]^-$ in the presence of a trace amount of H_2O.[15] It is therefore believed that the dianion $[SeFe_3(CO)_9]^{2-}$ is the initially formed product, which then transforms to the major product $[HSeFe_3(CO)_9]^-$.

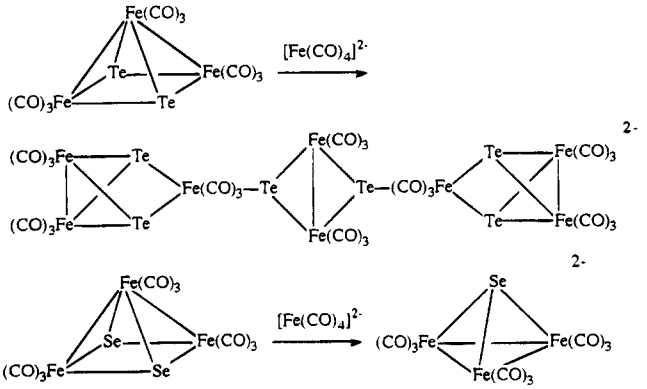

Structures of the Anionic Complexes II−IV. The anion of $[Et_4N]$[**II**] displays a $SeFe_2Co$ tetrahedral geometry in which the iron and cobalt atoms are pseudooctahedrally coordinated. A diagram showing the structure and labeling for the anion **II** is shown in Figure 1. The acute angles in $[Et_4N]$[**II**] about the basal atoms range from 55.82 to 59.95°, and those about selenium atom average 68.21°, which deviates a bit from a perfect tetrahedral geometry. The electron count for the cluster anion **II** is conventional. The mixed metal anion **II** is structurally related to clusters $SeFeCo_2(CO)_9$ and $TeFeCo_2(CO)_9$.[20] **II** is isostructural and isoelectronic with both of these.

(19) Shieh, M.; Chen, P.-F.; Peng, S.-M.; Lee, G.-H. *Inorg. Chem.* **1993**, *32*, 3389.
(20) Strouse, C. E.; Dahl, L. F. *J. Am. Chem. Soc.* **1971**, *93*, 6032.

Table 6. Selected Bond Distances (Å) and Bond Angles (deg) for $[Et_4N][Te_2Fe_2Mn(CO)_{10}]$ ($[Et_4N]$[**III**])

(A) Distances: Metal−Metal Bond Lengths			
Te(1)−Te(2)	3.207(2)	Te(1)−Fe(1)	2.593(1)
Te(1)−Fe(2)	2.573(1)	Te(1)−Mn	2.680(1)
Te(2)−Fe(1)	2.590(2)	Te(2)−Fe(2)	2.595(1)
Te(2)−Mn	2.689(1)	Fe(1)−Fe(2)	2.575(2)
(B) Angles			
Te(2)−Te(1)−Fe(1)	51.74(3)	Te(2)−Te(1)−Fe(2)	51.94(3)
Te(2)−Te(1)−Mn	53.45(3)	Fe(1)−Te(1)−Fe(2)	59.79(4)
Fe(1)−Te(1)−Mn	96.64(4)	Fe(2)−Te(1)−Mn	97.21(4)
Te(1)−Te(2)−Fe(1)	51.81(3)	Te(1)−Te(2)−Fe(2)	51.34(3)
Te(1)−Te(2)−Mn	53.19(3)	Fe(1)−Te(2)−Fe(2)	59.55(4)
Fe(1)−Te(2)−Mn	96.48(4)	Fe(2)−Te(2)−Mn	96.48(4)
Te(1)−Fe(1)−Te(2)	76.46(4)	Te(1)−Fe(1)−Fe(2)	59.73(4)
Te(2)−Fe(1)−Fe(2)	60.31(4)	Te(1)−Fe(2)−Te(2)	76.72(4)
Te(1)−Fe(2)−Fe(1)	60.48(4)	Te(2)−Fe(2)−Fe(1)	60.14(4)
Te(1)−Mn−Te(2)	73.36(4)		

Table 7. Selected Bond Distances (Å) and Bond Angles (deg) for $[Et_4N][Se_2Fe_2Mn(CO)_9]$ ($[Et_4N]$[**IV**]) (Where M = $^1/_2$Mn + $^1/_2$Fe)

(A) Distances: Metal−Metal Bond Lengths			
Se(1)−Se(2)	3.119(1)	Se(1)−M(1)	2.395(1)
Se(1)−M(2)	2.373(1)	Se(1)−Fe(3)	2.385(1)
Se(2)−M(1)	2.396(1)	Se(2)−M(2)	2.376(1)
Se(2)−Fe(3)	2.386(1)	M(1)−Fe(3)	2.711(2)
M(2)−Fe(3)	2.620(2)		
(B) Angles			
Se(2)−Se(1)−M(1)	49.39(3)	Se(2)−Se(1)−M(2)	48.98(3)
Se(2)−Se(1)−Fe(3)	49.20(3)	M(1)−Se(1)−M(2)	97.82(5)
M(1)−Se(1)−Fe(3)	69.11(4)	M(2)−Se(1)−Fe(3)	66.81(4)
Se(1)−Se(2)−M(1)	49.37(3)	Se(1)−Se(2)−M(2)	48.90(3)
Se(1)−Se(2)−Fe(3)	49.17(3)	M(1)−Se(2)−M(2)	97.72(5)
M(1)−Se(2)−Fe(3)	69.08(4)	M(2)−Se(2)−Fe(3)	66.75(4)
Se(1)−M(1)−Se(2)	81.25(4)	Se(1)−M(1)−Fe(3)	55.28(4)
Se(2)−M(1)−Fe(3)	55.30(4)	Se(1)−M(2)−Se(2)	82.12(4)
Se(1)−M(2)−Fe(3)	56.82(4)	Se(2)−M(2)−Fe(3)	56.82(4)
Se(1)−Fe(3)−Se(2)	81.64(4)	Se(1)−Fe(3)−M(1)	55.62(4)
Se(1)−Fe(3)−M(2)	56.37(4)	Se(2)−Fe(3)−M(1)	55.62(4)
Se(2)−Fe(3)−M(2)	56.43(4)	M(1)−Fe(3)−M(2)	84.75(5)

As shown in Figure 2, the anion of $[Et_4N]$[**III**] exhibits a $Te_2Fe_2(CO)_6$ butterfly with a $[Mn(CO)_4]^-$ fragment bridging the Te atoms. The Te_2Fe_2Mn core adopts the structure predicted for a five-vertex *arachno*-cluster. The Te(1)−Te(2) distance of 3.207(2) Å is indicative of the absence of direct bonding; however, intramolecular interaction may be significant.[4] The average Te−Fe distance in $[Et_4N]$[**III**] is 2.588 Å. This compares well to those in some related tellurium−iron carbonyl clusters such as 2.590 Å in $[PhCH_2NMe_3]_2[Te_6Fe_8(CO)_{24}]$,[19] 2.520 Å in $Fe_2(CO)_6(\mu\text{-}TeCHCl_2)_2$,[21] 2.541 Å in $Fe_2(CO)_6(\mu\text{-}TeCHPhTe)$,[21] 2.525 Å in $Fe_2(CO)_6(\mu\text{-}TeCH_2CH_2Te)$,[22] 2.535 Å in $Fe_2(CO)_6(\mu\text{-}TeCH_2CH_2CH_2Te)$,[22] 2.544 Å in $[Et_4N][BrTe_2Fe_2(CO)_6]$,[22] 2.549 Å in $Fe_2(CO)_6(\mu\text{-}TeCH_2Te)$,[23] 2.53 Å in $Te_2Fe_3(CO)_9$,[24] and 2.602 Å in $Te_2Fe_3(CO)_9(PPh_3)$.[7] The structurally characterized complexes with the *arachno*-Te_2M_3 framework are also seen in $Te_2Fe_3(CO)_9(PPh_3)$,[7] $Te_2Mo_2Fe(CO)_7Cp_2$,[4] $Te_2Fe_2(CO)_7(RhCp)$,[25] and $Te_2Fe_2(CO)_6M(PPh_3)_2$ (M = Ni, Pt, Pd).[8,9]

$[Et_4N]$[**IV**] exhibits a square-pyramidal Se_2Fe_2Mn metal core with an apical Fe atom and trans Se atoms. The iron and manganese atoms in the base are disordered. The selenium−selenium distance of 3.119(1) Å is regarded formally as nonbonding.[26] The bond lengths of Se(1)−Fe(3) and Se(2)−Fe(3) average 2.3855 Å and are normal. The Se_2FeMn base is not an ideal planar. Within the "square" base, angles at the selenium atom are obtuse (M(1)−Se(1)−M(2) = 97.82(5)° and M(1)−Se(2)−M(2) = 97.72(5)°, where M = $^1/_2$Fe + $^1/_2$Mn) while those about the iron and manganese atoms are acute (Se(1)−M(1)−Se(2) = 81.25(4)° and Se(1)−M(2)−Se(2) = 82.12(4)°, where M = $^1/_2$Fe + $^1/_2$Mn). The atoms of Se_2M_2 square have a mean deviation from the plane of 0.082 Å. The structure of the anion **IV** and its atomic numbering scheme are presented in Figure 3.

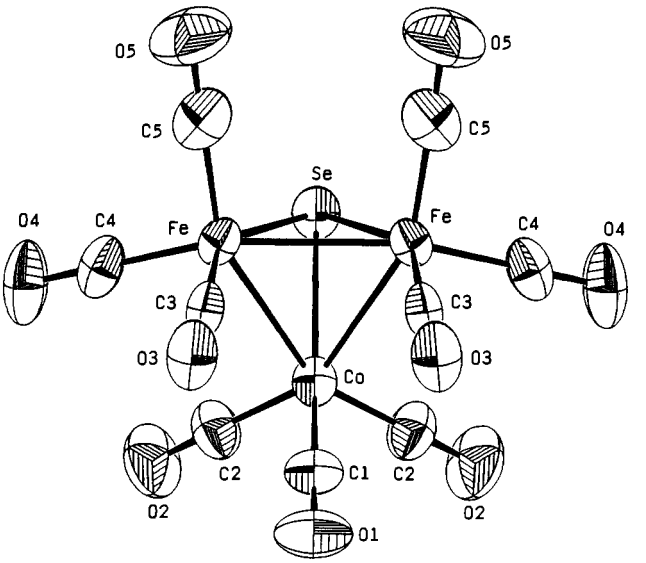

Figure 1. ORTEP diagram showing the structure and atom labeling for the anion of $[Et_4N][SeFe_2Co(CO)_9]$ ($[Et_4N]$[**II**]).

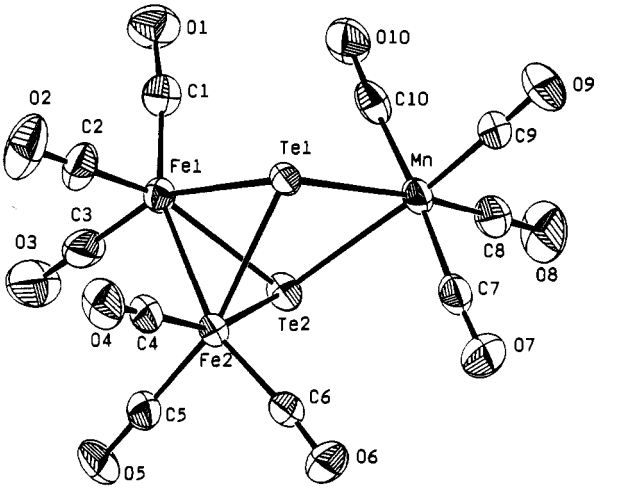

Figure 2. ORTEP diagram showing the structure and atom labeling for the anion of $[Et_4N][Te_2Fe_2Mn(CO)_{10}]$ ($[Et_4N]$[**III**]).

The core geometry of $[Et_4N]$[**IV**] is consistent with Wade's rule for a five-vertex *nido*-cluster containing seven skeletal bonding pairs. This cluster anion is structurally closed to the square-pyramidal neutral cluster $Se_2Fe_3(CO)_9$[27] except that one $Fe(CO)_3$ vertex of the base is replaced by a $[Mn(CO)_3]^-$ fragment. The selenium−iron distances of $[Et_4N]$[**IV**] average 2.3858 Å. This is comparable to the average distances in

(21) Shieh, M.; Chen, P.-F.; Tsai, Y.-C.; Shieh, M.-H.; Peng, S. M.; Lee, G.-H. *Inorg. Chem.* **1995**, *34*, 2251.
(22) Shieh, M.; Shieh, M.-H. *Organometallics* **1994**, *13*, 920.
(23) (a) Mathur, P.; Reddy, V. D. *J. Organomet. Chem.* **1991**, *401*, 339. (b) Mathur, P.; Reddy, V. D. *J. Organomet. Chem.* **1990**, *387*, 193.
(24) Schumann, H.; Magerstädt, M.; Pickardt, J. *J. Organomet. Chem.* **1982**, *240*, 407.
(25) Lesch, D. A.; Rauchfuss, T. B. *Inorg. Chem.* **1983**, *22*, 1854.
(26) (a) McConnachie, J. M.; Ibers, J. A. *Inorg. Chem.* **1991**, *30*, 1770. (b) Wolmershäuer, G.; Heckmann, G. *Angew. Chem., Int. Ed. Engl.* **1992**, *31*, 779. (c) Kanatzidis, M. G. *Comments Inorg. Chem.* **1990**, *10*, 161.
(27) Dahl, L. F.; Shutton, P. W. *Inorg. Chem.* **1963**, *2*, 1067.

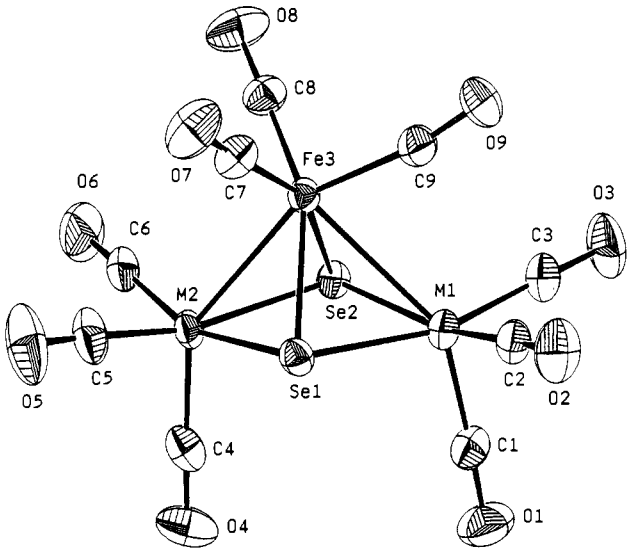

Figure 3. ORTEP diagram showing the structure and atom labeling for the anion of $[Et_4N][Se_2Fe_2Mn(CO)_9]$ ($[Et_4N]$[**IV**]) (where M = $^1/_2$Mn + $^1/_2$Fe).

$Se_2Fe_3(CO)_9$ (2.35 (1) Å),[27] $Se_2Fe_2(CO)_6$ (2.364 (11) Å),[28] $[\{Se_2Fe_2(CO)_6\}_2(Se_2)]^{2-}$ (2.39 (2) Å),[29] and $[\{SeFe_3(CO)_9\}_2Hg]^{2-}$ (2.311 Å).[10] $[Et_4N]$[**IV**] is isoelectronic and isostructural with the known molecules such as $M_2Fe_3(CO)_9$ (M = S, Se, Te, AsPh, SO).[24,27,30-32]

One important feature of the anionic clusters **I**–**IV** worth mentioning is that they represent four examples of chalcogen-containing mixed transition-metal anionic clusters. The introductions of a second kind of transition-metal fragment into selenium–iron and tellurium–iron carbonyl clusters are very successful in these cases, and these methodologies may provide facile routes to the modification of cluster frameworks.

Discussion

The previous study has indicated that most metal–metal exchange reactions are mechanistically complex.[33] It has shown that the nature of metal–metal bonds and the stability of the intermediates and/or products are usually the key controlling factors in these types of reactions.[34,35] The reactions of $E_2Fe_3(CO)_9$ (E = Te, Se) with $[Co(CO)_4]^-$, $[Mn(CO)_5]^-$, and $[Fe(CO)_4]^{2-}$ are, therefore, of particular interest with regard to the roles of the main-group and transition elements.

Cluster Formation. It has been shown that the chalcogen atoms of $E_2Fe_3(CO)_9$ (E = S, Se, Te) readily add the unsaturated transition-metal center $M(PPh_3)_2$ (M = Ni, Pd, Pt) followed by loss of one iron vertex each to give the metal-bridging butterfly complex.[8,9,36] Unlike the previous reports, the tetrahedral $[EFe_2Co(CO)_9]^-$ (E = Se, Te) complexes were obtained from the reactions of $E_2Fe_3(CO)_9$ with $[Co(CO)_4]^-$. This result may imply that the two chalcogen atoms are not susceptible to be attacked by the incoming anion $[Co(CO)_4]^-$ and the observed tetrahedral products may result from complicated bond breakage and formation processes.

In analogy with the reactions with the low-valence metal complexes, the reaction of $Te_2Fe_3(CO)_9$ with $[Mn(CO)_5]^-$ forms an *arachno*-Te_2Fe_2Mn cluster anion **III**. Taking advantages of these facts, one can propose the formation of **III** involving the oxidative addition of the $[Mn(CO)_5]^-$ across the Te atoms of $Te_2Fe_3(CO)_9$ with the loss of one CO group and the elimination of one $Fe(CO)_3$ fragment. Similarly, the formation of **IV** may involve the straightforward additions of two Se–Mn bonds and one additional Mn–Fe bond. In this case, it is believed that the shorter Se–Mn distances could facilitate the Mn–Fe bond formation to yield a more closed *nido*-square pyramidal cluster.

The reactions with $[Fe(CO)_4]^{2-}$ seem to undergo complicated bond rearrangements to give $[Te_6Fe_8(CO)_{24}]^{2-}$ and $[SeFe_3(CO)_9]^{2-}$, respectively. Since the analogous cluster $[TeFe_3(CO)_9]^{2-}$ has been isolated in the Te–Fe–CO system,[2h,14,21] it suggests that the reaction of $Te_2Fe_3(CO)_9$ with $[Fe(CO)_4]^{2-}$ may proceed via $[TeFe_3(CO)_9]^{2-}$ to form $[Te_6Fe_8(CO)_{24}]^{2-}$. However, $[TeFe_3(CO)_9]^{2-}$ may be unstable under this reaction condition and $[Te_6Fe_8(CO)_{24}]^{2-}$ and $[SeFe_3(CO)_9]^{2-}$ are the thermally stable products for these two systems, respectively. As suggested by the observation of hypervalent bonding modes in some related tellurium complexes,[7,4,23] the hypervalency of tellurium may play a key role in the formation of the cluster $[Te_6Fe_8(CO)_{24}]^{2-}$. Schmid has suggested that the ease of formation of bonds between the transition metals in transition-metal–main-group clusters is related to the size of the main-group and transition elements.[37] These different outcomes also tend to agree with Schmid's statement in terms of the greater size of tellurium (1.35 Å) and similar sizes for the selenium (1.17 Å) and iron (1.25 Å).[38,39]

Effects on Cluster Formation. The distances of the *trans* chalcogen atoms in the original clusters $E_2Fe_3(CO)_9$ (E = Te, Se) are 3.36 and 3.10 Å,[4,27] respectively. The cobalt carbonyl group does not bridge across the *trans* chalcogen atoms, presumably, due to the long chalcogen–chalcogen distances and the small size of cobalt atom (1.26 Å).[39] Furthermore, it has been demonstrated that the general weakness of the metal–metal or metal–heavy-atom-ligand bonds usually accounts for the metal–metal breakage and metal-scrambling processes.[40] Thus, the metal–metal or metal–main-group bond of $E_2Fe_3(CO)_9$ (E = Te, Se) could be easily broken by the incoming anion, which leads to the cluster reconstruction and results in the *closo*-clusters **I** and **II** caused by the favorable Fe–Fe and Fe–Co bond formation due to the similar sizes of iron (1.25 Å)[39] and cobalt (1.26 Å).

We have noted the Te···Te distance of 3.207(2) Å in cluster **III**, close to that of a similar cluster $Cp_2Mo_2FeTe_2(CO)_7$ (3.14 Å), shows no formal Te–Te bond; however, a certain degree of intramolecular interaction is proposed.[4] The main-group–main-group interaction has been proposed to play an important role in the formation of $Cp_2Mo_2FeTe_2(CO)_7$ from $Te_2Fe_3(CO)_9$.[4] Our result tends to support this hypothesis. Notably, the main-group–main-group contact is not sufficient enough to induce

(28) Campana, C. F.; Lo, F. Y.-K.; Dahl, L. F. *Inorg. Chem.* **1979**, *18*, 3060.
(29) Huang, S.-P.; Kanatzidis, M. G. *Inorg. Chem.* **1993**, *32*, 821.
(30) Wei, C. H.; Dahl, L. F. *Inorg. Chem.* **1965**, *4*, 493.
(31) Jacob, W.; Weiss, E. *J. Organomet. Chem.* **1977**, *131*, 263.
(32) Markó, L.; Markó-Monostory, B.; Madach, T.; Vahrenkamp, H. *Angew. Chem., Int. Ed. Engl.* **1980**, *19*, 226.
(33) Shriver, D. F.; Kaesz, H. D.; Adams, R. D. *The Chemistry of Metal Cluster Complexes*; VCH Publishers: New York, 1990.
(34) (a) Vahrenkamp, H. *Adv. Organomet. Chem.* **1983**, *22*, 169. (b) Blumhofer, R.; Fischer, K.; Vahrenkamp, H. *Chem. Ber.* **1986**, *119*, 194. (c) Mani, D.; Vahrenkamp, H. *Chem. Ber.* **1986**, *119*, 3639. (d) Beaurich, H.; Vahrenkamp, H. *Angew. Chem., Int. Ed. Engl.* **1981**, *20*, 98. (e) Blumhofer, R.; Fischer, K.; Vahrenkamp, H. *Chem. Ber.* **1986**, *119*, 194. (f) Vahrenkamp, H. *Comments Inorg. Chem.* **1985**, *4*, 253.
(35) Knight, J.; Mays, M. J. *J. Chem. Soc., Dalton Trans.* **1972**, 1022.
(36) Mathur, P.; Mavunkal, I. J. *Inorg. Chim. Acta* **1987**, *126*, L9.
(37) Schmid, G. *Angew. Chem., Int. Ed. Engl.* **1978**, *17*, 392.
(38) Huheey, J. E.; Keiter, E. A.; Keiter, R. L. *Inorganic Chemistry: Principles of Structure and Reactivity*; Harper Collins College Publishers: New York, 1993.
(39) Dahl, L. F.; Rodulfo de Gil, E.; Feltham, R. D. *J. Am. Chem. Soc.* **1969**, *91*, 1655.
(40) Müller, M.; Schacht, H.-T.; Fischer, K.; Ensling, J.; Gütlich, P.; Vahrenkamp, H. *Inorg. Chem.* **1986**, *25*, 4032.

the formation of an *arachno*-cluster in the analogous reaction with $Se_2Fe_3(CO)_9$. For **IV**, the release of strain in $Se_2Fe_3(CO)_9$ is probably not as important as that in $Te_2Fe_3(CO)_9$. In support of this view, it has been known that $Se_2Fe_3(CO)_9$, unlike $Te_2Fe_3(CO)_9$, does not form an *arachno*-adduct with PPh_3.[4,6]

As in many metal cluster reduction reactions,[33] the severe bond rearrangement in the case of $Te_2Fe_3(CO)_9$ with $[Fe(CO)_4]^{2-}$ may be induced by the introduction of the electron sources,which is evidenced by the formation of $[Te_6Fe_8(CO)_{24}]^{2-}$ in about the same yield from the reaction of $Te_2Fe_3(CO)_9$ with 2 equiv of cobaltocene.[21] Similar observation is also seen in the reaction of $Se_2Fe_3(CO)_9$ with $[Fe(CO)_4]^{2-}$.[15] This outcome contrasts a previous study[41] by Whitmire and co-workers which indicates that $Bi_2Fe_3(CO)_9$ maintains its original metal skeleton in the reaction with $[Fe(CO)_4]^{2-}$ because of the basicity requirement. The differences may be ascribed to the differing electronic demands for the main-group elements in group 15 and 16. In summary, the reactions of $E_2Fe_3(CO)_9$ (E = Te, Se) with $[Co(CO)_4]^-$ give the *closo*-$[EFe_2Co(CO)_9]^-$ complexes whereas those with $[Mn(CO)_5]^-$ form an *arachno*-$[Te_2Fe_2Mn(CO)_{10}]^-$ and a *nido*-$[Se_2Fe_2Mn(CO)_9]^-$, respectively. The formation of these products can be rationalized in terms of the metal−metal, metal−main-group, and main-group−main-group interactions. On the other hand, the reactions with $[Fe(CO)_4]^{2-}$ proceed with complex cluster rearrangements presumably due to the charge and the size effects.

(41) Whitmire, K. H.; Raghuveer, K. S.; Churchill, M. R.; Fettinger, J. C.; See, R. F. *J. Am. Chem. Soc.* **1986**, *108*, 2778.

Conclusion

The key effects which determine the formation of metal clusters are difficult to probe owing to the complicated metal−metal breakage and formation. From the study of the parallel reactions of $E_2Fe_3(CO)_9$ (E = Se, Te) with a series of transition-metal complexes, the formation of mixed-transition-metal chalcogenides can be rationalized in terms of size, basicity, bonding nature, and charge effects of the chalcogen atoms and the transition elements. This work sheds some light on the roles of main-group and transition metals in cluster formation and provides facile routes to mixed-transition-metal chalcogenides. The information should be valuable in the synthesis and design of other main-group-containing mixed-metal carbonyl clusters.

Acknowledgment. We thank the National Science Council of the Republic of China for financial support (Grant Nos. NSC 83-0208-M-003-004 and NSC 84-2113-M-003-008).

Supplementary Material Available: Complete listings of crystallographic data, atomic positional and thermal parameters, bond distances and angles, and anisotropic thermal parameters (12 pages). Ordering information is given on any current masthead page.

IC941279L